Nat. Hazards Earth Syst. Sci., 26, 3253–3272, 2026
https://doi.org/10.5194/nhess-26-3253-2026

Natural Hazards and Earth System Sciences
Open Access
EGU

Feature selection for landslide forecasting models in Southern Andes

Manuel Labbé[1], **Millaray Curilem**[1], **Ivo Fustos-Toribio**[2], **and Mario Pooley**[2]

[1]Department of Electrical Engineering, Universidad de La Frontera, Temuco, Chile
[2]Department of Civil Engineering, Universidad de La Frontera, Temuco, Chile

Correspondence: Ivo Fustos-Toribio (ivo.fustos@ufrontera.cl)

Received: 11 June 2025 – Discussion started: 30 June 2025
Revised: 1 April 2026 – Accepted: 25 June 2026 – Published: 14 July 2026

Abstract. Rainfall-induced landslides (RIL) are a major hazard in the Southern Andes, threatening lives, infrastructure, and ecosystems. Early warning systems require accurate predictive models; however, their effectiveness is constrained by heterogeneous data availability and the lack of universal design standards. This study develops a systematic framework to identify the most influential features controlling landslide generation by integrating local soil, climatic, and topographic datasets. A national landslide inventory was expanded using Buffer Control Sampling and PUBagging to improve the representation of non-landslide cases, yielding a robust database of 3148 instances with 136 variables. Feature selection was performed using Classification and Regression Trees (CART) and, in parallel, Genetic Algorithms (GA), with both approaches evaluated using Support Vector Machines, Random Forest, and XGBoost classifiers. Results highlight precipitation, slope, and soil hydraulic properties – particularly bulk density and saturated water content – as recurrent critical predictors. GA-based models significantly outperformed CART, with GA-RF and GA-XGB achieving the lowest error rates (10.95 %) while using compact feature sets. These findings underscore the potential of evolutionary feature selection to enhance predictive accuracy while reducing data complexity, and they provide actionable insights into which variables should be prioritised in monitoring networks. This work contributes to the design of more reliable and region-specific early warning systems for rainfall-induced landslides, emphasising the role of shallow and deep water storage features in mountainous environments.

1 Introduction

Rainfall-induced landslides (RIL) pose a significant threat to communities worldwide, causing loss of life, property damage, and disruption of essential infrastructure. RIL occurrence and magnitude are expected to intensify under changing climatic conditions, as alterations in precipitation regimes increase the likelihood of hydrologically driven slope failures. Despite substantial progress in landslide research, the development of reliable early warning systems that mitigate their effect is still under development due to limited data and the absence of standardised approaches for identifying the key environmental controls on slope instability. In this context, the present study advances a systematic methodology for determining the dominant features governing landslide initiation using as study case the Southern Andes. Establishing and quantifying these controlling variables is essential for improving monitoring strategies, enhancing predictive capabilities, and ultimately strengthening risk-reduction efforts in susceptible landscapes.

Recent studies have established that quantitative and data-driven methodologies markedly enhance the robustness and predictive skill of landslide models (Kumar et al., 2023; Merghadi et al., 2020). Within this framework, Steger et al. (2023) demonstrate that landslide forecasts are fundamentally constrained by the precision and representativeness of input data, showing that precipitation exerts seasonally variable controls on slope failure and therefore requires high-quality climatic observations. Complementary studies underscore the pivotal role of numerical simulations in landslide hazard assessment integrating geotechnical uncertainty to quantify the failure mechanisms and potential impacts (Jia et al., 2023; Fustos-Toribio et al., 2022, 2025). Moreover, hydrological modelling efforts further confirm the centrality of rainfall dynamics, with rainfall-driven frameworks demonstrating strong capability in the prediction of shallow landslides (Bezak et al., 2019). Collectively, these works highlight a critical need for methodological refinement that moves beyond broad variable inclusion and instead isolates the most influential features governing landslide initiation, thereby enabling the development of more accurate, transparent, and operationally meaningful predictive models.

Landslide generation is a complex, multi-variable process governed by the interplay of geological, climatic, and anthropogenic factors, with substantial spatial variability in the dominant controls (Chen et al., 2024; Fidan et al., 2024). Topography constitutes a primary conditioning factor; however, its influence can be subordinated by local subsurface dynamics, particularly rapid variations in soil moisture at specific depths, which are especially relevant in rainfall-triggered failures (Margaño-Carmona et al., 2025; Fustos-Toribio et al., 2025). Additional contributors such as lithology, drainage density, and structural discontinuities interact with triggering mechanisms – most notably intense or prolonged precipitation – to determine slope stability. Consequently, landslide susceptibility assessment becomes inherently challenging, as it must incorporate a large number of interdependent variables whose combined effects are difficult to disentangle (Margaño-Carmona et al., 2023; Zighmi et al., 2025). The central methodological difficulty lies in processing this heterogeneous information and isolating the variables that most strongly control landslide initiation.

Climate change further exacerbates this complexity. Increasing temperatures and shifts in precipitation regimes are already amplifying the frequency and intensity of hydrological extremes, elevating landslide hazard in susceptible regions (Crozier, 2010). Such dynamics are particularly evident in mountain belts like the Himalayas, where accelerated glacial melt and heightened rainfall intensity have led to pronounced increases in slope failures (Ballabh et al., 2014). At the same time, human-induced landscape alterations, including deforestation, urbanisation, and land-use change, destabilise natural soil structures and modify drainage networks, increasing the likelihood of failure under otherwise moderate hydrological forcing (Xu et al., 2024; Wang et al., 2023).

The convergence of these natural and anthropogenic drivers underscores the need for region-specific, data-driven approaches capable of distinguishing the most influential conditioning and triggering factors. Stand out the topographic influence in landslide susceptibility (Lin et al., 2017), meanwhile soil moisture emerges as a critical factor on a global scale, particularly in regions prone to rainfall-triggered landslides (Maragaño-Carmona et al., 2025). Additionally, geological characteristics such as lithology and drainage density are crucial conditioning factors that interact with triggering mechanisms like extreme precipitation events (Bisht and Rawat, 2023). Such precisions are essential for developing accurate, operationally relevant predictive models and for designing effective landslide early warning and risk-management strategies. To address this multi-variable complexity and enhance predictive accuracy, advanced methodologies must be combined with classification techniques, to refine model inputs and achieve more precise, actionable spatial predictions (Kumar et al., 2023; Ge et al., 2022).

Landslides in the Southern Andes are predominantly influenced by a combination of geological, climatic, and tectonic factors that interact to create a complex landscape prone to instability (Fustos-Toribio et al., 2021; Ochoa-Cornejo et al., 2025; Maragano-Carmona et al., 2025). The region's geological composition, characterised by steep slopes and diverse lithologies, plays a significant role in landslide susceptibility. Studies indicate that the presence of weak lithology along the margin and the geomorphological features could predispose areas to landslides, particularly during extreme precipitation events (Maragano-Carmona et al., 2025). Additionally, climatic factors, particularly rainfall, are pivotal in triggering landslides in the Southern Andes. Research has shown that intense and prolonged rainfall events significantly increase the likelihood of landslides, especially in areas lacking adequate drainage systems (Fustos-Toribio et al., 2022; Islam et al., 2021). The development of rainfall-induced landslide early warning systems (RILEWS) has been proposed as a means to mitigate the risks associated with these events. However, such systems are not yet operational in the Southern Andes (Fustos-Toribio et al., 2022). Furthermore, the interaction between vegetation and slope stability is also noteworthy; while vegetation can stabilise slopes, its removal or degradation can lead to increased landslide occurrences (Vorpahl et al., 2012).

To understand the impact of geomorphological, hydrological and geotechnical features in landslide susceptibility delimitation, machine learning (ML) has emerged as a pivotal tool, particularly in the development of regional susceptibility analysis or early warning systems (Merghadi et al., 2020; Fustos-Toribio et al., 2022). The complexity of landslide phenomena, influenced by various geological and climatic conditions, requires tailored approaches to make accurate predictions. Recent studies indicate that ML models, such as Support Vector Machines (SVM) (Huang et al., 2019), Random Forests (RF) (Park and Kim, 2019), and Extreme Gradient Boosting (XGB) (Yang et al., 2024), among others, outperform traditional statistical methods in terms of predictive accuracy and robustness (Li et al., 2019; Bravo-López et al., 2023). Approaches that integrate various ML techniques have been shown to enhance spatial agreement in mapping landslide susceptibility, thus improving the reliability of predictions (Adnan et al., 2020; Bravo-López et al., 2023). Feature selection plays a crucial role in optimising model performance by identifying the most relevant variables that contribute to landslide occurrences, thus reducing noise and enhancing interpretability (Halder et al., 2024; Ge et al., 2022; Pham et al., 2020). This not only improves classification performance but also provides keys to understanding the phenomenon and deciding which variables to monitor. Many strategies can be used to perform the selection: filter methods select features based on statistical criteria obtained from their individual behaviour while wrapper methods evaluate the contribution of feature subsets on the classification performance, finally, embedded methods perform feature selection internally during model training through algorithm-specific mechanisms related to the specific ML model (Theng and Bhoyar, 2024; Guyon and Elisseeff, 2003). Another important challenge is the definition of negative examples. Regional data scarcity complicates the development of ML models, and this limitation is exacerbated by the fact that available databases typically contain only positive cases, requiring negative samples to be defined empirically. Consequently, it becomes essential to adopt appropriate strategies to construct balanced datasets. Buffer Control Sampling and PUBagging (Positive-Unlabeled Bagging) has been effectively used to address this issue (Gu et al., 2024; Wu et al., 2021).

This manuscript presents a methodological framework to understand the complex and dynamic processes of landslide generation in the Southern Andes (38–42° S), employing for the first time a rigorous, data-driven methodology in this region. We aim to identify and delineate the key variables that must be considered in the Southern Andes to adequately characterise landslide triggering and controlling conditions. To improve the performance and explainability of the machine learning models, two feature-selection strategies were applied in parallel: a filter-based approach that ranks the features according to their importance, using Classification and Regression Trees (CART), and a wrapper-based approach employing Genetic Algorithms (GA) for feature-subset optimisation. Both strategies were evaluated using different classification techniques, enabling a detailed assessment of the relative importance of climatic variables, soil properties, and geological features. This targeted feature selection process is vital for identifying the true local critical factors that govern slope instability in this climatically active and geologically heterogeneous environment, effectively translating complex hydro-geomorphological processes into quantifiable variables. The prioritised factors are then strategically repurposed as high-quality proxies to refine and improve variable mapping, enabling a crucial regional-to-local scale approach that captures the spatial variability of landslide susceptibility. The provision of an in-depth, data-validated analysis of the critical variables that interplay among triggering mechanisms will support the design of next-generation, ML-based monitoring networks and accurate early warning systems (EWS) for this vulnerable mountain range.

2 Study zone

We consider a sparse data area, focused in the Southern Andes, spanning latitudes from 38 to 43° S (Fig. 1). The area presents a unique and complex geological and climatological landscape that significantly influences soil moisture dynamics and mass wasting processes. The diverse geological composition of the study area yields a complex landscape, formed by numerous relief changes related to volcanic and glacial processes during the Holocene and more recently, influenced by different-scale mass wasting processes (Maragaño-Carmona et al., 2025; Fustos-Toribio et al., 2022, 2025). From a geological perspective, the area has a wide range of lithological units, encompassing volcanic rocks (andesites, basalts), metamorphic rocks (Horton, 2018), sedimentary formations, and glacial deposits (Cuzzone et al., 2024). This variability introduces potential soil sources from weathered rocks and sediment sources that will send their material to sedimentary environments to the subduction area along the central valley. However, the amount of the source is still poorly quantified.

The geological framework of the Southern Andes is predominantly shaped by tectonic activity, resulting in a range of rock types, including andesites, basalts, and sedimentary rocks. Stand out the volcanic activity, where this area contributed to volcanic eruptions, ranging from plinian to strombolian, which formed tephra deposits with different mineralogies (Moreno-Yaeger et al., 2024). The tephra degradation during the Holocene triggered high soil variability, characterised by different textures and water retention capacities, which could control the landslide triggering processes. Moreover, the different soil textures generated from lithological and tephra deposits control the water storage and the following organic matter content.

The area was covered by two pulses of glacial periods (Cuzzone et al., 2024), which modified the relief and eroded previous deposits leaving young soils prone to be affected by landslides on the eastern side. Meanwhile, ancient soils are present in the western area, creating a good contrast between soil ages. The presence of glacial deposits from the last glacial maximum has resulted in the formation of heterogeneous soil profiles, which vary in texture and composition throughout the region (Vásquez-Antipán et al., 2025). These features influence the water retention and drainage properties, thereby affecting soil moisture levels and slope susceptibility to mass wasting events. Understanding the main control of the soil features becomes essential for assessing the stability of slopes and predicting potential landslide occurrences. In addition to the wide range of lithological and soil properties and features existing in the area, the climate of the Southern Andes exhibits an extreme range of climates, from arid to humid, influenced by altitude, latitude, and patterns of western winds and atmospheric rivers (Tetzner et al., 2025). The main precipitation amount occurs primarily in the austral winter months (May–September), reaching over 4000 mm yr^{-1}. The summer dry seasons modify soil moisture dynamics at different depths, with an unknown impact on landslides. Recently, climate change has posed additional challenges, as shifts in precipitation patterns and increased

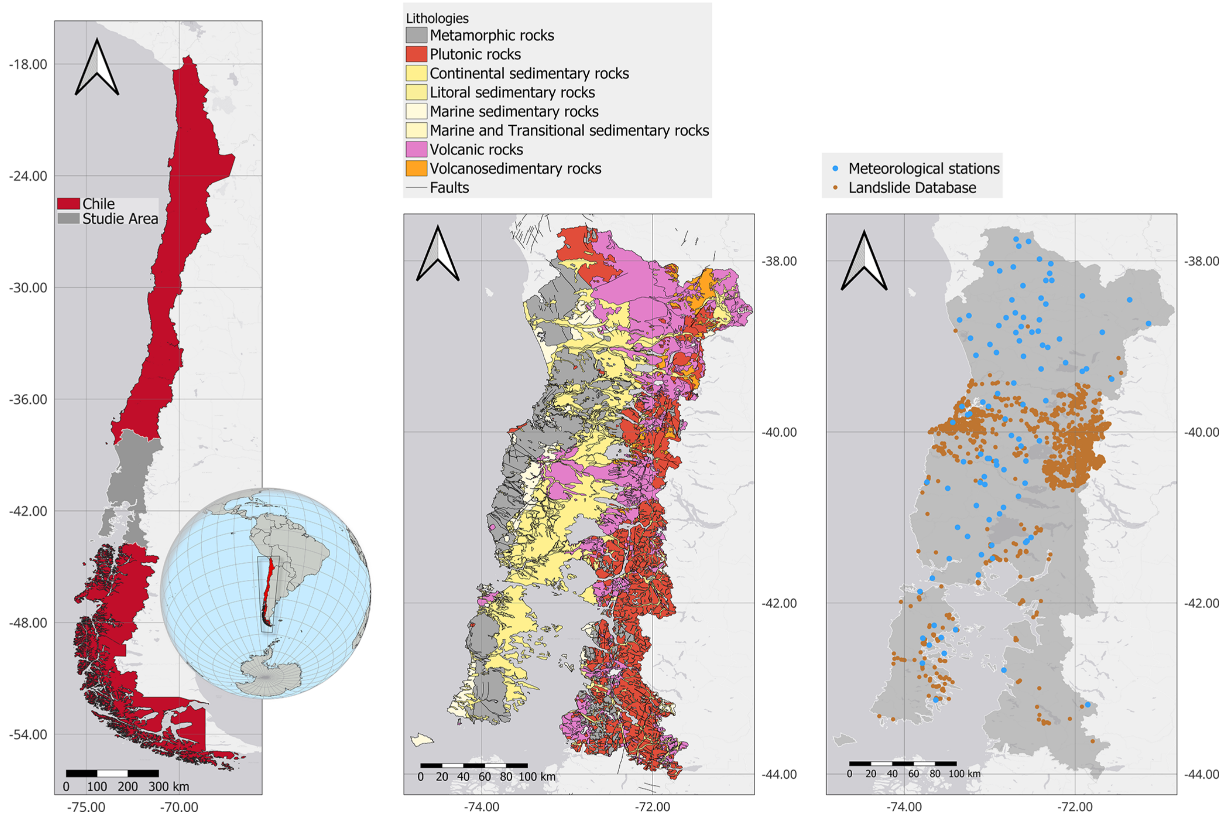

Figure 1. Study zone. Left: National-scale map indicating the spatial coverage of the database. Middle: Zoom to study zone with geology as background, showing the heterogeneity of media in this study. Right: Rainfall-induced landslide (orange) and weather stations (blue) demonstrating the reduced spatial coverage.

frequency of extreme weather events may exacerbate soil erosion and landslide risks.

Nowadays, accurately assessing landslide risk in this region presents significant challenges. The high variability in multiple variables introduces a complex dynamic that acts as a primary control on slope stability, which is currently poorly understood. The interplay of these varying variables creates a highly dynamic environment where the key relationships governing stability can change dramatically over short distances. The study area has been affected by large-scale mass wasting events (Fustos-Toribio et al., 2021; Ochoa-Cornejo et al., 2025; Maragano-Carmona et al., 2025; Vásquez-Antipán et al., 2025), underscoring the need to develop a robust early warning system and enhance assessment accuracy. This requires comprehensive, integrated studies to create models that fully incorporate geological, climatic, and soil data, including the often-overlooked parametric controls, enabling a reliable landslide early warning system. A network of advanced sensors is needed to monitor real-time changes in all the variables across the varying lithological units. However, it needs to focus on the main variables, which have not yet been established.

3 Database

To assess the interplay between rainfall intensity, soil moisture, and geological factors that underlie landslide occurrences, it is essential to construct a comprehensive and reliable database. We designed and developed databases that synthesise data sets, including meteorological records, modelled soil moisture, and detailed hydraulic soil properties. We used an approach to identify critical conditioning factors that could be systematically captured and quantified, providing a solid empirical foundation for subsequent machine-learning-based risk assessments using soil features extracted from high-resolution Chilean databases via pixel-to-point processing (Dinamarca et al., 2023). The generated database enabled constraining the soil features to the exact emplacement of the landslide and its date, considering the lithological and climatic features within the study area. The selection allowed capture the range of soil and lithologic features under different hydrometeorological and climatic conditions in the Southern Andes. The selected data provided a robust framework for analysing the dynamic relationships between hydrological, geological, and climatic controls in landslide generation.

We considered the soil moisture, precipitation (PP), and slope from the ERA5 database (ERA5, 2023), one of the most widely used climate datasets, with 10 km resolution. The slope was obtained by combining the ERA5 database with high-resolution digital elevation models from the shuttle Radar Topography Mission (SRTM), at 30 m spatial resolution (NASA JPL, 2013). The Chilean soil properties were extracted from the CLSoilMaps database (Dinamarca et al., 2023). The ERA5-Land dataset corresponds to the land component of the European Centre for Medium-Range Weather Forecasts' (ECMWF) fifth-generation reanalysis, executed under the Copernicus Climate Change Service (C3S) mandate, being generated via offline, high-resolution integrations of the ECMWF land surface model, CHTESSEL. The offline generation approach offers improved temporal consistency in land surface fields, thereby representing global water and energy cycles more accurately (Muñoz-Sabater et al., 2021). The dataset delivers approximately 50 variables essential for describing hydrological and surface energy processes, including soil moisture, runoff, snow cover, skin temperature, evapotranspiration, and land carbon fluxes at high resolution, providing a 9 km global horizontal resolution in comparison to 31 and 80 km resolutions of ERA5 and ERA-Interim, respectively. The currently accessible public record spans from January 1981 to the present, subject to a typical latency of 2–3 months. To mitigate boundary discontinuities, each stream is preceded by multi-year spin-up periods. However, residual inconsistencies are acknowledged, particularly within variables with long memory, such as deep soil moisture and permanent snow regions. The internal consistency of ERA5-Land is intrinsically tied to its reliance on ERA5 for meteorological forcing, through a 4D-Var data assimilation system. Near-surface air temperature, pressure, and humidity are, however, corrected for elevation discrepancies between the ERA5 and ERA5-Land grids utilising daily lapse rates. Validation against diverse observational datasets, including in situ networks, satellite products, and hydrological records, unequivocally demonstrates that ERA5-Land surpasses ERA5 performance in the representation of soil moisture, temperature, runoff, and lake dynamics (Muñoz-Sabater et al., 2021; Bonshoms et al., 2022; Yilmaz, 2023). Moreover, we utilised the new CLSoilMaps database, an improvement over global soil databases in Chile. CLSoilMaps provides spatially explicit and high-resolution predictions of critical soil physical and hydraulic properties specifically for continental Chile and its shared transboundary basins with Argentina. The database was rigorously developed using Digital Soil Mapping (DSM) techniques within the SCORPAN framework (McBratney et al., 2003), trained on over 4000 soil profile observations that encompass diverse and historically underrepresented ecosystems, including those in the Andes and Patagonia. Modelled soil attributes include clay, sand, and bulk density, with silt content derived indirectly from these parameters. Hydraulic properties, such as field capacity, permanent wilting point, and available water capacity, were estimated using the well-established Rosetta V3 pedotransfer function (Zhang and Schaap, 2017). The predictions were executed using Random Forest algorithms that incorporated over 200 environmental covariates, spanning climate, topography, and satellite-based reflectance indices, and adhered to the six standardised depth intervals (0–200 cm) stipulated by the GlobalSoilMap project.

We used a rainfall-induced landslide database developed using the Xterrae database (https://www.xterrae.cl/, last access: 1 June 2024) maintained by the National Geology and Mining Service (SERNAGEOMIN) of Chile. Positive landslide events were obtained from this source, while negative cases were generated using a Buffer Control Sampling strategy (Gu et al., 2024). In this approach, a buffer zone of 100 m was established around each landslide event, and sampling points were extended outward up to a 20 km radius. This distance was intentionally chosen given the 10 km resolution of the climatological variables, enabling the capture of spatial variability of the precipitation and soil moisture content, differentiating between landslide and non-landslide conditions. Subsequent refinement of the negative examples was performed via a modified PUBagging (Gu et al., 2024), built on the idea of bagging (bootstrap aggregating) by repeatedly sampling subsets of the unlabeled data and combining them with the positive set to train multiple base classifiers. In our setting, many candidate negative samples can exhibit characteristics that are very similar to the positives, and including them could make the decision boundary more difficult to find and the classification unnecessarily more complex. PUBagging provides a way to mitigate this risk by leveraging the positive set and treating each subset as if the unlabeled instances were negative (which may introduce noise), and by aggregating the predictions across many such classifiers, PUBagging reduces the bias introduced by this assumption and improves robustness. The final decision is typically made through majority voting or averaging across these classifiers. Here a Random Forest model – trained exclusively on positive examples – was used to evaluate the negative cases. Negative instances yielding a prediction score above 0.5 were removed, ensuring a more robust set of non-landslide cases.

After excluding records with missing values from the initial 3388 entries, the final database comprises 3148 examples, including 1618 positive and 1530 negative instances. Each record contains 136 normalised feature columns and an additional column indicating binary landslide occurrence. Although explicit vegetation indices, such as NDVI, were not included in the dataset, vegetation effects are implicitly incorporated through predicted soil properties influenced by NDVI measurements, reflecting parameters such as organic matter content and soil moisture. Notably, approximately 95 % of the data is concentrated in the Los Lagos and Los Ríos regions, resulting in a regionally focused dataset for subsequent analysis.

Table 1. List of Variables available in the databases. AvMoist: Available moisture = $\theta_{FC} - \theta_{PWP}$ (cm^3 cm^{-3}); AWC: Available water capacity (mm); Bulk: bulk density of the fine fraction (g cm^{-3}); Clay/Silt/Sand: textural fractions (%); FC: field capacity at 330 kPa (cm^3 cm^{-3}); PWP: permanent wilting point at 1500 Kpa (cm^3 cm^{-3}); θ_s: saturated water content (cm^3 cm^{-3}); θ_r: residual water content (cm^3 cm^{-3}); k_{sa}: saturated hydraulic conductivity (cm d^{-1}); n, α: van Genuchten shape parameters (–, cm^{-1}); Vmoist: volumetric soil moisture (cm^3 cm^{-3}); PP: precipitation (mm); slope: terrain slope (degrees); Tex_Class: soil textural class (%); PIRange_X: prediction-interval range for property X (_Bulk: g cm^{-3}; _Clay: %; _Sand: %); Total_AWC: depth-integrated AWC (mm).

File abbreviation	Description	unit
α	"alpha" shape parameter (SD)	1 cm
AvMoist	Available Moisture at FC-PWP	cm^3 cm^{-3}
AWC	Available water capacity at FC-PWP	mm
Bulk	bulk density of the fine fraction	g cm^{-3}
Clay	Clay content	%
FC	Field capacity at 330 kPa	cm^3 cm^{-3}
k_{sa}	saturated hydraulic conductivity	cm d^{-1}
n	"n" shape parameter	–
PIRange_Bulk	prediction intervals for Bulk density	g cm^{-3}
PIRange_Clay	prediction intervals for clay properties	%
PIRange_Sand	prediction intervals for sand properties	%
PP	Daily precipitation	mm
PWP	Permanent wilting point at 15 000 kPa	cm^3 cm^{-3}
Sand	Sand content	%
Silt	Silt content	%
slope	slope	°
Tex_Class	soil textural classes	%
θ_r	residual water content	cm^3 cm^{-3}
θ_s	saturated water content	cm^3 cm^{-3}
Total_AWC	Sum of AWC across all depths	mm
VMoist	Moisture value	cm^3 cm^{-3}

Table 2. Symbols used to represent the soil variables designation. Depth suffixes: a = 0–5 cm; b = 5–15 cm; c = 15–30 cm; d = 30–60 cm; e = 60–100 cm; f = 100–200 cm. An underscore "_" denotes the mean across depths; a dot "." denotes the standard deviation.

Symbol	Depth
a	0–5 cm
b	5–15 cm
c	15–30 cm
d	30–60 cm
e	60–100 cm
f	100–200 cm
_	Mean vealue
.	standard deviation

4 Methodology

Here, we present the methodology used to examine the relationships between rainfall intensity, soil moisture, and soil characteristics in rainfall-induced landslide generation, to support the development of robust monitoring networks and reliable early warning systems for landslides, as well as to identify the most significant variables. First, highly correlated variables were removed from the initial database. Then, both filter and a wrapper parallel feature selection strategies were applied. Finally, optimised data sets were used to design the landslide classifiers. All this process is shown in Fig. 2.

The CART-based filter method ranks variables based on their individual discriminatory power between positive and negative cases. In contrast, the GA-based wrapper approach optimises a subset of features by evaluating their combined contribution to classification performance. In this case, the genetic algorithm evolves to find the best feature combination that minimises an objective function (Katoch et al., 2020). This objective function was designed to reduce the number of selected variables and the classifier error, evaluated using three models: Support Vector Machines, Random Forest, and XGB. The filter and the wrapper strategies were independently evaluated by assessing the quality of the optimised datasets through the performance of the classifiers, ensuring a consistent estimation of the relevance of each contributing variable.

4.1 Correlation analysis

Before performing the feature selection and because several features measure the same variable at different depths, it was necessary to perform a correlation analysis to remove the more correlated variables (Fig. 2). Eliminating corre-

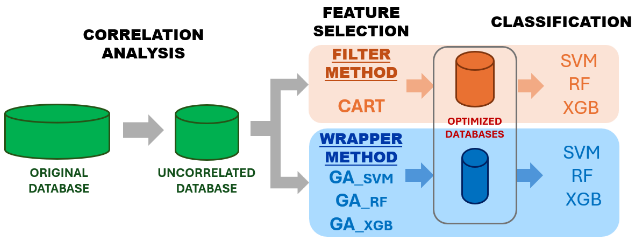

Figure 2. General methodology to identify the most relevant variables in landslide estimation: first, correlated variables are removed. Then, two feature selection methods (Filter and Wrapper) are applied. Finally, different classifiers are trained and validated using the selected features. The best subsets of features are obtained from the best classifiers performance.

lated variables in machine learning allows to reduce redundant information, which increases model complexity without adding information. Moreover, high correlation may cause issues like multicollinearity in linear models, leading to unstable coefficients, increasing the risk of overfitting and hiding the importance of other features, thus negatively affecting generalisation.

Figure 3 presents the correlation map of the complete database, with variables ordered according to Table 1 with their different depths. Figure 4 shows the correlation values of the remaining variables after removing highly correlated features. As shown in Fig. 3, strong correlations are observed within subgroups of variables at different depths, as well as between average moisture (AvMoist) and available water capacity (AWC), among others. From the initial set of 136 features, applying a correlation threshold of |0.9| resulted in the removal of 83 highly correlated variables, yielding a reduced set of 53 features for subsequent filter- and wrapper-based selection. The remaining variables are listed in Table 3.

4.2 Feature Selection

The core of this study lies in feature selection, aiming to identify the most influential variables involved in landslide generation in the Southern Andes. Feature selection reduces model complexity, accelerates training, enhances generalisation, and improves interpretability while mitigating overfitting (Ge et al., 2022; Ebrahimi Warkiani and Moattar, 2025; Zheng and Casari, 2021). To ensure robustness and consistency, we adopt redundant feature selection procedures considering both filter and wrapper methods (Song et al., 2025). As stated before, the filter method is based on CART while the wrapper method assesses through GA feature subsets collectively, leveraging classifier performance to guide selection.

4.2.1 CART filter method

This method was applied to filter out less significant variables in the estimation model by recursively partitioning the

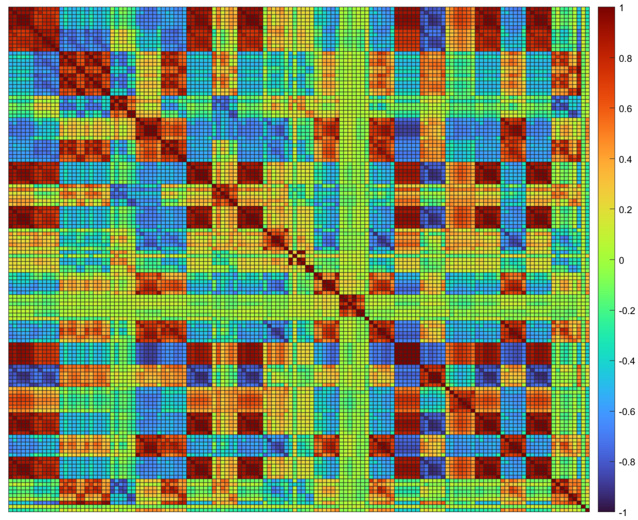

Figure 3. Correlation matrix of the 136 variables, highlighting groups of redundant features, some of them due to the same variables measured at different depths. All the variables are listed in Tables 1 and 2.

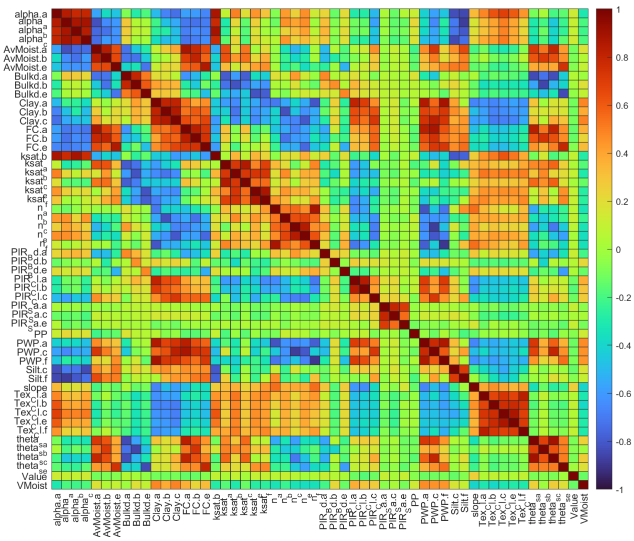

Figure 4. Correlation matrix for the 53 less correlated variables (correlation under the threshold of |0.9|). These less correlated variables are presented in Table 3.

data set using a decision tree algorithm (Fig. 5). Each node in the resulting tree is split based on the feature that best separates the data into distinct classes, ranking variables according to their individual contribution to accurate classification. In the CART-based filtering strategy, the variables that appear deeper in the decision tree are considered less significant, being split into fewer samples than those selected near the root. Consequently, these lower-ranked features can be discarded to retain only the most significant ones. However, while CART effectively identifies and ranks individual fea-

Table 3. List of the 53 less correlated variables that remained after the correlation filtering process. The correlation threshold was |0.9|.

α.a	Clay.a	k_{sat}_e	PIR_Cl.a	Silt.c	θs_c
α_a	Clay.b	k_{sat}_f	PIR_Cl.b	Silt.f	θs_e
α_b	Clay.c	n_a	PIR_Cl.c	slope	VMoist
α_c	FC.a	n_b	PIR_Sa.a	Tex_Cl.a	
AvMoist.a	FC.b	n_c	PIR_Sa.c	Tex_Cl.b	
AvMoist.b	FC.e	n_e	PIR_Sa.e	Tex_Cl.c	
AvMoist.e	k_{sat}.b	n_f	PP	Tex_Cl.e	
Bulkd.a	k_{sat}_a	PIR_Bd.a	PWP.a	Tex_Cl.f	
Bulkd.b	k_{sat}_b	PIR_Bd.b	PWP.c	θ_{s}_a	
Bulkd.e	k_{sat}_c	PIR_Bd.e	PWP.f	θ_{s}_b	

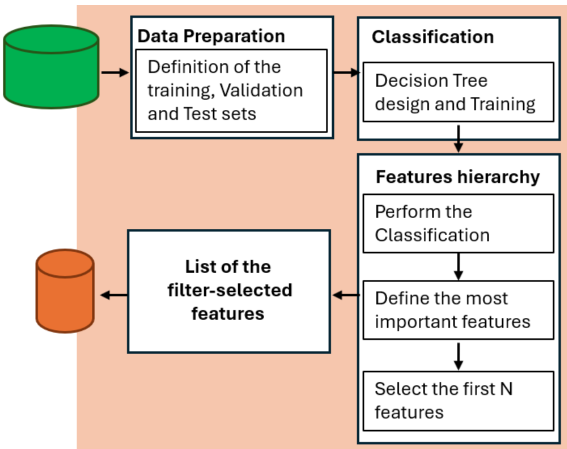

Figure 5. Filter method: general structure of the CART feature selection process. First the database is prepared and the Decision Tree is trained using the global database. The features are sorted based on their importance scores obtained in the training process. A threshold is defined to retain the top features. At the end of the process a new dataset is created, containing only the CART selected top features.

tures, it does not assess the combined contribution of multiple variables.

The Gini Index (or Gini Impurity) metric was used to split the database (Eq. 1). An assessment of the pure dataset at a node during the tree-building process was carried out. It supports the split at each step selecting the features allowing to reduce the impurity in the decision nodes.

$$\mathrm{Gini} = 1 - \sum_{k=1}^{C} p_k^2 \tag{1}$$

Equation (1) has p_k that represents the proportion of samples in a node that belong to class k, and C is the number of classes (two in this case). The Gini Index ranges from 0 (a pure node, where all samples belong to one class) to 0.5 (maximum impurity for binary classification, where samples are evenly distributed between the two classes). Finally, the importance of each feature is calculated as the average of the impurity reductions it achieves across all the nodes in the model.

The CART design involves tuning seven hyperparameters. The maximum depth of the tree is adjusted with discrete values: 200 max_depth $\in \{3, 4, 5, 6, 7, 8, 10, 12, 15\}$. The minimum number of samples to divide the data set, and the minimum number of leaves of the separation, are defined with min_samples_split $\in \{2, 3, 4, 5, 7, 10, 15, 20\}$ and min_samples_leaf $\in \{1, 2, 3, 4, 5, 7, 10\}$, respectively. The maximum number of features considered at each split, max_features, is chosen from {sqrt,log2,none}. If None, then nodes are expanded until all leaves are pure or until all leaves contain less samples than min_samples_split. Additionally, class_weight balances class weights, the minimum fraction of a leaf is set as min_weight_fraction_le $\{0, 0.1, 0.2, 0.3\}$, and the minimum impurity reduction is defined as min_impurity_decrease $\in \{0, 0.01, 0.05, 0.1\}$.

4.2.2 GA wrapper method

Genetic algorithms are optimisation techniques inspired by natural selection, where an evolution process improves a set of solutions over successive generations. The process begins with a random initial population of potential solutions represented as "chromosomes", each formed by a set of encoded parameters called genes. These solutions are evaluated using a fitness function, which measures how well they perform on the target task. After evaluation, the fittest solutions of each generation have a greater chance of being selected to "reproduce", using genetic operators like crossover (combination of the chromosomes) and mutation (randomly altering a gene). These operators introduce variation, which allows the algorithm to explore new parts of the solution space. Over multiple generations, less optimal solutions are naturally discarded and the population evolves toward the best solution. In the present study, the chromosome is defined as a sequence of M bits, where M is the number of features remaining after correlation (53 features) and each location in the chromosome corresponds to a specific feature. A 1 in location m indicates that this feature will be considered in the classifier design, while a zero indicates the absence of

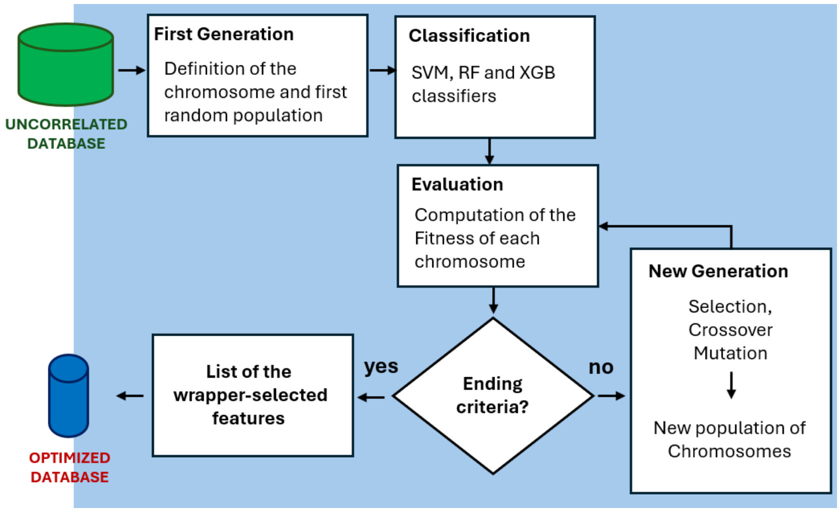

Figure 6. Wrapper method: general structure of the GA feature selection process. The process begins with a population of randomly generated feature subsets, which are used to train classifiers and evaluate their performance. While the stopping criteria are not met, a new population is generated based on the performance of the previous generation, and the evaluation process is repeated. The process continues until either the optimal performance is achieved or the maximum number of generations is reached. At the end of the process, the output is a database containing the wrapper optimised feature subset.

this feature. At the beginning the values of the chromosomes of the first population were random, so each chromosome proposes a random combination of the features. The evaluation of the chromosomes (that is, the evaluation of the feature combinations) is carried out using a fitness function, which assigns a fitness value to each chromosome. In this study, the fitness value is derived from the classification error and an additional penalty term that discourages the selection of large feature sets. This formulation forces the GA to seek optimal classification performance using a reduced number of variables, thereby simplifying the models and identifying the most relevant features. The fitness value assigned to each chromosome is given by Eq. (2). The classifiers were implemented using SVM, RF and XGB. The general structure of the GA feature selector is presented in Fig. 6.

$$\text{FitnessValue} = \text{Error} + \frac{N_{\text{SF}}}{100} \quad (2)$$

where N_{SF} is the number of selected features for a chromosome. The Error index is calculated as expressed in Eq. (3).

$$\text{Error} = \frac{\text{FP} + \text{FN}}{N} \quad (3)$$

where FP are the false positive landslides, while FN are the false negative, that is the non detected landslides and N the total number of examples.

The performance of a genetic algorithm depends on the careful tuning of its hyperparameters. In this study, the population size was set to 50 chromosomes, ensuring sufficient genetic diversity to explore the solution space effectively. The algorithm was allowed to evolve for a maximum of 300 generations, providing ample opportunity for convergence toward an optimal feature subset. For the selection mechanism, we employed tournament selection with a tournament size of 3, favoring fitter chromosomes while maintaining selection pressure. Crossover was performed using a two-point crossover method, in which two parent chromosomes are randomly selected and genetic material between two crossover points is exchanged to produce two offspring. The crossover probability P_{Cros} defines the likelihood that a pair of chromosomes undergoes crossover. Mutation, which introduces random variability and helps prevent premature convergence, was controlled by the mutation probability P_{Mut} and a bit-flip probability P_{Flip}, which governs the likelihood of flipping individual bits within a chromosome. The overall probability of a bit being mutated is calculated using Eq. (4).

$$P_{\text{BitMutation}} = P_{\text{Mut}} \times P_{\text{Fplip}} \quad (4)$$

Finally, we implemented an operator to maintain a record of the best individuals across generations (set to the four best individuals), ensuring that high quality solutions are preserved throughout the evolutionary process. The crossover (P_{Cros}), mutation (P_{Mut}) and flip (P_{Flip}) probabilities were set in a trial and error method by exploring values in the range of 0.2 to 0.9, with increments of 0.1, where each evolution was performed with different values and the best fitness defined which probabilities were the best ones. The genetic algorithm was then executed multiple independent runs to reduce the risk of premature convergence or local optima.

4.3 Classification Methods

To estimate rainfall-induced landslides (RIL), classifiers were developed using the feature sets obtained from both the filter and wrapper selection methods. In the case of the CART-based filter method, classifiers served solely to evaluate the predictive power of the preselected features. However, in the wrapper-based approach, classifiers played a dual role: they acted both as the objective function guiding the genetic algorithm's optimisation and as the evaluators of each candidate feature subset's performance. This dual function required the implementation, training, and comparison of over a thousand models to identify the most effective feature combination.

The study systematically developed and refined several SVM, RF and XGB classifier models. For each model type, a grid search was employed to explore a range of hyperparameters, and three-fold cross-validation was used to evaluate model performance and mitigate the risk of overfitting. The subsequent sections provide a comprehensive description of the model 255 configurations and the methodological criteria for feature selection.

4.3.1 Support Vector Machine

SVMs are classification algorithms that find the best-separating hyperplane in high-dimensional space, handling nonlinear data with kernel functions. They are effective for small to moderate datasets with many features, offering good control over overfitting through regularisation. However, they are computationally expensive for large datasets and harder to interpret than the tree-based methods. Our SVM classifier was designed using 3-fold cross-validation and required tuning two hyperparameters: the cost constant $C = 2^{\alpha}$, where $\alpha \in [-5, 8]$, which controls the trade-off between empirical error and classifier complexity; and the RBF kernel width $\sigma = 2^{\beta}$, where $\beta \in [-7, 5]$, which was adjusted for the Gaussian function.

4.3.2 Random Forest

RF classifiers are designed using an ensemble of decision trees with bagging to improve model accuracy and robustness to overfitting. The RF model was tuned with 9 hyperparameters: number of trees (n_estimators $\in \{100, 200, 300, 500\}$), maximum depth (max_depth $\in \{3, 5, 7, 10, 15, 20\}$), minimum samples to split (min_samples_split $\in \{2, 5, 10, 15, 20\}$) and leaf (min_samples_leaf $\in \{1, 2, 4, 6, 8\}$), maximum features max_features, is chosen from { sqrt, log2, all}, maximum leaves (max_leaf $\in \{50, 100, 200\}$), minimum weight fraction (min_weight_fraction_leaf $\in \{0.0, 0.1, 0.2\}$), and minimum impurity reduction (min_impurity_decrease $\in \{0, 0.01, 0.05\}$). We evaluated bootstrapping and non bootstrapping strategies to build the trees.

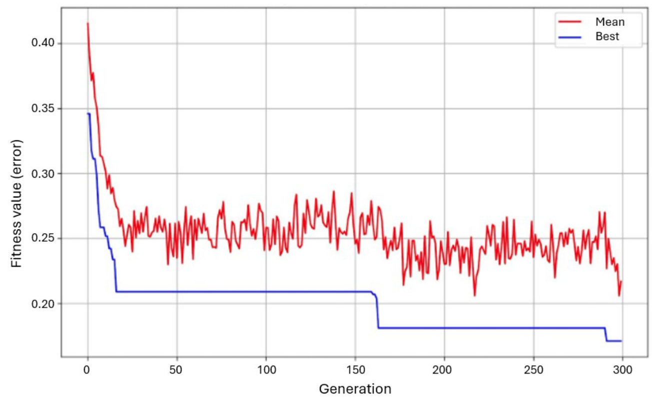

Figure 7. Genetic Algorithm Convergence: the curves show the population's average performance (Mean) and the best individual's performance (Best) across an evolution of 300 generations.

4.3.3 Extreme Gradient Boosting

XGB model was designed to capture subtle relationships between variables, leveraging its strengths in handling large datasets and complex interactions. The XGB model was tuned with 7 key hyperparameters: number of trees n_estimators $\in \{100, 200, 300, 500\}$), maximum depth (max_depth $\in \{3, 5, 7, 9, 11, 13\}$), minimum child weight (min_child_weight $\in \{1, 3, 5, 7\}$), minimum loss reduction (gamma $\in \{0, 0.1, 0.2, 0.3, 0.4\}$), learning rate (learning_rate $\in \{0.01, 0.05, 0.1, 0.15, 0.2\}$), L1 regularisation term (reg_alpha $\in \{0, 0.1, 0.5, 1.0\}$), and L2 regularisation term (reg_lambda $\in \{0.1, 0.5, 1.0, 1.5, 2.0\}$). These hyperparameters were optimised to balance model complexity and prevent overfitting, ensuring the XGB model performed accurately and robustly.

5 Results

To understand the relationship between rainfall intensity, soil moisture, and soil hydraulic features in landslide generation, we present an in-depth analysis of the conditioning factors that influence landslide occurrence in a region of the southern Andes (38–42° S). After exploring various machine learning models with different feature configurations, we observed notable differences in performance depending on the features subsets. This process helped identify which combinations of features and modeling approaches best captured the underlying structure of the data. The results reveal that the dynamic interactions among rainfall intensity, soil moisture patterns, and geological characteristics are significant at the determined exploration depth of the soil, based on the database used during feature selection. The following section presents the results, highlighting the most promising models and the impact of feature selection on the performance of susceptibility estimation.

Table 4. Results of the evolution: best sets of variables obtained for each evolution according to the classifier and their best errors obtained on the test set.

Discriminator	Parameters	Hyperparameters	Feature Selection	Best Error (%)
CART	P_{Cros}: – P_{Mut}: – P_{Flip}: –	max_depth: 15 min_samples_split: 4 min_ samples_leaf: 1 max_features: None class_weight: balanced min_weight_ fraction_leaf: 0.0 min_impurity_decrease: 0.0	AvMoist.a, Clay.b, Clay.c, k_{sat}_e, PIRange_Bulkd.b, PIRange_Bulkd.e, PIRange_Clay.c, PIRange_Sand.c, PIRange_Sand.e, PP, n_a, n_c, slope, θ_s_e, VMoist	26.67 ± 3.45
GA_SVM	P_{Cros}: 0.8 P_{Mut}: 0.2 P_{Flip}: 0.5	C: 2 σ: 0.125	α.a, AvMoist.e, Clay.a, PIR_Cl.c, PP, slope, θ_s_b, VMoist	21.98 ± 3.39
GA_RF	P_{Cros}: 0.6 P_{Mut}: 0.3 P_{Flip}: 0.3	n_estimators: 200 max_depth: 20 min_samples_split: 2 min_ samples_leaf: 1 max_features: sqrt min_weight_fraction_leaf: 0.0 min_impurity_decrease: 0.0 bootstrap: True	Bulkd.b, k_{sat}_a, PP, PWP.f, slope, VMoist	10.95 ± 2.44
GA_XGB	P_{Cros}: 0.8 P_{Mut}: 0.3 P_{Flip}: 0.5	n_estimators: 500 max_depth: 7 min_child_weight: 1 gamma: 0.0 learning_rate: 0.2 reg_alpha: 0 reg_lambda: 0.5	Bulkd.b, n_b, n_f, PP, Tex_Class.f, slope, θ_s_a, θ_s_c, VMoist	10.95 ± 2.44

5.1 Feature selection

The results presented in Table 4 show differing model performance across classifiers and feature selection methods. The CART approach achieved its best error rate of 26.67 % using a relatively large feature set of 15 variables, including swallowing variables such as the average moisture at 0–5 cm, clay content at 5–15 cm and slope. In contrast, the GA-based feature selection methods (GA-SVM, GA-RF, and GA-XGB) delivered improved performance using fewer features. Figure 7 illustrates an example of the GA-RF convergence over 300 generations, while Fig. 8 presents the most active features throughout this evolutionary process.

Both GA-RF and GA-XGB achieved the lowest error rates of 10.95 %, with 6 and 9 features, respectively. Common to both models were the consideration of slope and precipitation variables. At the same time, GA-RF also included shallow variables such as bulk density at 5–15 cm and available moisture. The feature selection using GA-XGB proposed the use of shallow variables at 5–15 cm of bulk density of the fine fraction and the shape parameter of the retention curve and saturated water content (θ_{s}). The GA-SVM method achieved an error rate of 21.98 % using 8 features, and selected variables such as the Van Genuchten parameter at 0–5 cm, Average moisture at 60–100 cm, and slope.

There is some overlap in the features selected by GA-RF and GA-XGB – both models include precipitation, slope, Volumetric moisture, and shallow bulk density (5–15 cm), suggesting that these are key indicators for rainfall-induced landslide assessment. However, differences in feature sets indicate distinct modelling perspectives. GA-RF uniquely selected saturated hydraulic conductivity at the first centimetre (0–5 cm) and depth of Permanent wilting point at 100–200 cm, pointing to a focus on near-surface hydraulic behaviour and deeper root-zone water retention. In contrast, GA-XGB favoured variables like shape parameter of SWRC at 5–15 and 100–200 cm, soil textural classes at 100–200 cm, and saturated water content at 0–5 and 15–30 cm, suggesting a broader interest in soil texture and porosity across both shallow and deep layers.

Compared to the CART approach, the GA-based methods selected more compact and targeted feature sets while delivering superior predictive performance. While CART relied on a larger number of features, GA-RF and GA-XGB focused on key physical properties such as slope and Bulkd.b, which are highly relevant for landslide modeling. These findings highlight the strength of GA-based wrapper feature selection, capturing the interactions between variables, isolating the most meaningful and in our case enhancing landslide

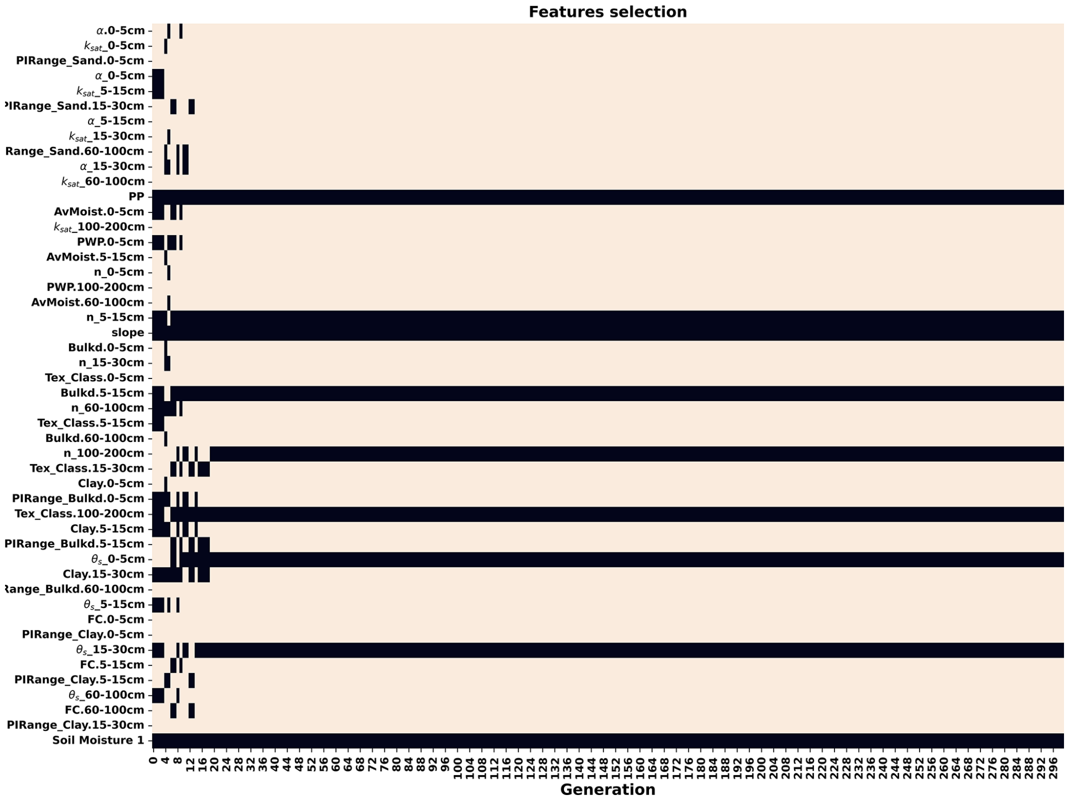

Figure 8. Feature selection evolution: most selected features across an evolution of 300 generations.

prediction accuracy by leveraging both shallow and deep soil characteristics.

5.2 Classification

The features selected by the different methods were used to train and test classifiers implemented with the three models – SVM, RF and XGB – to compare them. The results are presented in Table 5, providing a comprehensive overview of their performance under two distinct conditions: Non PUBagging and PUBagging. The evaluation metrics include accuracy and recall with their respective confidence intervals, both of which are critical for assessing the effectiveness of these classification models. Table 5 shows that the best-performing model in terms of recall was the one obtained using the features selected through GA-RF. The SVM achieved an accuracy of 0.735 with a confidence interval of ± 0.029, and a recall of 0.749 ± 0.041. The XGB model outperformed the SVM, recording an accuracy of 0.873 ± 0.020 and a recall of 0.885 ± 0.028, indicating its strong predictive capability. The Random Forest classifier exhibited the highest performance among the three models, achieving an accuracy of 0.879 ± 0.020 and a recall of 0.901 ± 0.027.

A Wilcoxon signed-rank test showed that the difference between RF and SVM – both with and without PUBagging – is statistically significant (p-value $= 1.23 \times 10^{-27}$). In contrast, no significant difference was observed between RF and XGB under either sampling strategy (p-value > 0.56). These findings indicate that all classifiers were effective in identifying landslide and non-landslide instances, with Random Forest and XGBoost consistently demonstrating the strongest overall performance. Moreover, the comparison between PUBagging and Non–PUBagging strategies revealed no statistically significant differences, suggesting that PUBagging did not substantially alter the classifiers' general predictive ability.

The superior performance of RF and XGB further highlights their effectiveness in capturing complex, nonlinear relationships within the dataset. Although GA-based optimisation improved all models, SVM appears less capable of fully exploiting such optimisation when compared to the more flexible and expressive structures of RF and XGB. Previous studies indicate that SVMs can perform competitively on simpler datasets but tend to lose effectiveness in more heterogeneous or high-dimensional contexts unless subjected to extensive parameter optimisation or trained on larger datasets. The recall results reinforce this interpretation, as RF and XGB achieve higher recall than SVM, indicating a stronger ability to minimise false negatives. This characteristic is particularly critical in applications where the identification of true positive cases – such as potential rainfall-induced landslides – is essential for early warning and risk mitigation.

Figure 9 presents RIL estimation in an example map of the Chilean study regions, showing how ML systems can support the identification of risk zones in landslide early-warning applications.

6 Discussion

Accurate landslide forecasting enables early warnings, allowing authorities and communities to take preventive measures, such as evacuations or slope stabilisation, to reduce risk. It also supports better land-use planning and disaster preparedness, contributing to long-term resilience against geological hazards. Ultimately, landslide forecasting is a critical tool for safeguarding lives and promoting sustainable development in high-risk areas. For the first phase of feature selection, expert analysis was considered, along with setting a correlation elimination threshold of |0.9|. Subsequently, two strategies were employed to finalise the feature selection: CART and a Genetic Algorithm.

6.1 Main controls in mass wasting generation

The accurate determination of parameters to monitor in rainfall-induced landslides is critical for effective risk assessment and management. As rainfall is a primary trigger for landslides, understanding the hydrological and geotechnical factors that influence slope stability is essential. Studies have shown that specific topographic parameters, such as slope angle, soil moisture content, and rainfall intensity, significantly correlate with landslide occurrences (Emberson et al., 2022; Novellino et al., 2021).

For instance, the integration of machine learning techniques with hydrological data has enhanced the predictive capabilities of landslide susceptibility models, allowing for a more nuanced understanding of how varying rainfall patterns affect slope stability (Novellino et al., 2021; Mondini et al., 2023). Moreover, the identification of key parameters is not only vital for immediate hazard assessment but also for long-term monitoring and mitigation strategies. Research indicates that rainfall anomalies and their spatial patterns can provide insights into potential landslide activity, thereby facilitating timely interventions (Marc et al., 2016; Wang et al., 2020). The dynamic nature of rainfall events necessitates continuous monitoring of these parameters to adaptively manage landslide risks, especially in regions prone to extreme weather conditions (Bordoni et al., 2015; Yang et al., 2024). Furthermore, the application of remote sensing technologies has proven effective in capturing real-time data on rainfall and its impact on slope stability, thus improving the accuracy of landslide predictions (Kirschbaum and Stanley, 2018; Gariano et al., 2015).

Our results allowed us to identify the recurrent variables related to rainfall-induced landslides in the Southern Andes. Specifically, we observed that precipitation, slope, and volumetric moisture (VMoist) are repeatedly selected features (Table 4). This recurrence suggests that these parameters capture key underlying characteristics crucial to achieving robust predictive performance. In particular, the consistency of these features across standard decision tree approaches and genetic algorithm–enhanced methods indicates their stability and high predictive relevance. Our results show consistency with the particular conditions of the Southern Andes, where the interaction between volumetric moisture (VMoist) and slope angle significantly influences landslide generation by affecting the shear strength and stability of the soil mass. High VMoist indicates near-saturated soil conditions, which lead to increased pore water pressures and a reduction in matric suction. These hydrological effects decrease the effective stress in the soil, thereby reducing its shear strength – a critical factor that predisposes slopes to failure. In regions with steep slopes, the gravitational forces acting downslope are significantly heightened, amplifying the destabilising effects of high moisture content, such as San Jose de Maipo (Maragaño-Carmona et al., 2023), Osorno Volcano (Fustos-Toribio et al., 2022) and Villa Santa Lucia (Somos-Valenzuela et al., 2020; Ochoa-Cornejo et al., 2025).

Another key variable selected by the automatic feature selection allowed for the reflection of the central control of the Southern Andes. The soil moisture contents in the 0–5 cm layer showed a critical variable in initiating infiltration when rainfall impacts these layers. These automatic selection shows concordance with the processes of water movement control proposed by Maragaño-Carmona et al. (2023), where high moisture content significantly influences local pore water pressures, a factor that has been directly linked to reduced shear strength and slope failure (Fustos-Toribio et al., 2025). Our results suggest considering the incorporation of depth-specific measurements to ensure that the models capture both the rapid near-surface processes and the more delayed responses in the underlying zones.

A physical interpretation of these findings in the Southern Andes suggests that the initiation of RIL in the study zone depends not only on rainfall magnitude, but also on the transient hydrological evolution of the soil profile being consistent with previous studies (Somos-Valenzuela et al., 2020; Maragaño-Carmona et al., 2025; Ochoa et al., 2025). Volumetric water content in the first layer (0–5 cm) provides information on antecedent wetness and remaining storage capacity (Nielsen et al., 2019; Peranić et al., 2022), while bulk density conditions the pore structure, compaction state, and permeability that regulate how water is absorbed and redistributed (Barnhart et al., 2025). The parameters related to the soil water retention curve define how moisture changes are translated into suction loss, thereby controlling the transition from unsaturated to near-saturated conditions (Oh et al., 2015). Together, these variables describe the sequence through which rainfall infiltrates, storage capacity is progressively exhausted, matric suction is reduced, and pore pressure response becomes more likely. Monitoring these features in

Table 5. Results for Non PUBagging and PUBagging models with different discriminators, best results shown in bold.

Discriminator	Database	Classifier	Accuracy	Recall
CART	No PUBagging	SVM	0.740 ± 0.043	0.781 ± 0.058
		XGB	0.860 ± 0.036	0.877 ± 0.045
		RF	0.800 ± 0.039	0.830 ± 0.049
	PUBagging	SVM	0.763 ± 0.045	0.809 ± 0.057
		XGB	**0.862 ± 0.035**	0.880 ± 0.046
		RF	0.835 ± 0.039	**0.889 ± 0.044**
GA-SVM	No PUBagging	SVM	0.783 ± 0.026	0.812 ± 0.034
		XGB	**0.880 ± 0.021**	0.887 ± 0.028
		RF	0.875 ± 0.021	0.883 ± 0.029
	PUBagging	SVM	0.791 ± 0.025	0.835 ± 0.032
		XGB	0.870 ± 0.021	0.874 ± 0.029
		RF	0.876 ± 0.021	**0.890 ± 0.027**
GA-RF	No PUBagging	SVM	0.735 ± 0.029	0.749 ± 0.041
		XGB	0.873 ± 0.020	0.885 ± 0.028
		RF	**0.879 ± 0.020**	**0.901 ± 0.027**
	PUBagging	SVM	0.769 ± 0.028	0.809 ± 0.037
		XGB	0.862 ± 0.022	0.889 ± 0.028
		RF	0.856 ± 0.023	0.881 ± 0.028
GA-XGB	No PUBagging	SVM	0.759 ± 0.027	0.795 ± 0.037
		XGB	0.875 ± 0.021	**0.889 ± 0.028**
		RF	0.861 ± 0.021	0.881 ± 0.029
	PUBagging	SVM	0.781 ± 0.025	0.786 ± 0.034
		XGB	**0.896 ± 0.019**	0.886 ± 0.026
		RF	0.873 ± 0.021	0.872 ± 0.030

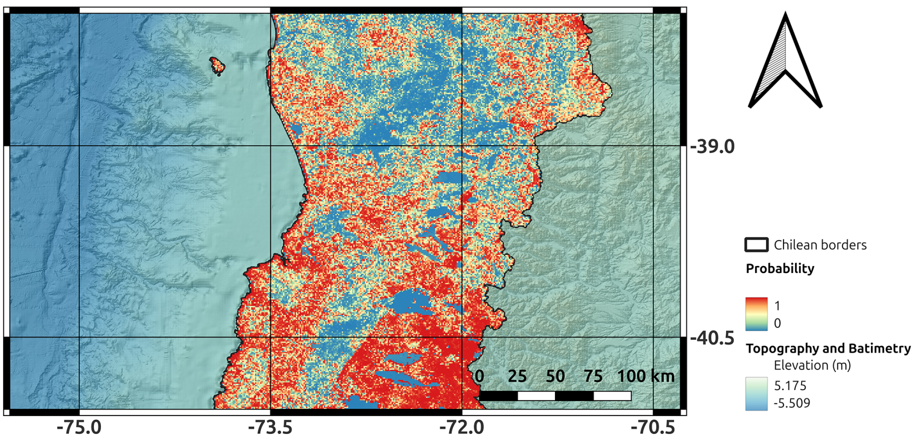

Figure 9. Example Probability of RIL in the Southern Chile Area.

operational monitoring networks could provide a physically meaningful framework for tracking slope destabilization, because it allows the identification of the progression from early infiltration to near-surface saturation and, eventually, to the hydromechanical conditions that favor shallow slope initiation. Rather than acting as isolated predictors, these variables collectively could represent the physical slope response during rainfall events, offering support for process-based interpretation and early warning applications if in the future this features are monitored or constrained in high susceptible areas.

6.2 Lesson learned about classification

Using a selection features approach, we performed a susceptibility landslide assessment focused on the Southern Andes (Table 5). Our results generated a landslide susceptibility modelling considering the depth-dependent heterogeneity of soil properties and their impact on the landslide controls. The use of different classifiers (e.g., CART, GA-SVM, GA-RF, GA-XGB) with tuned hyperparameters attests to the complexity of modelling the interaction between multilayered soil properties and water infiltration dynamics. An accurate selection of features from various depths helps to predict transient hydrological responses, for example, rapid saturation of near-surface layers followed by a more gradual moisture redistribution in deeper layers (Maragano-Carmona et al., 2025). Our results allowed us to constrain the data necessary to perform landslide susceptibility for the Southern Andes, if required, at a better scale into the future. We interpret the results of the selected features into the landslide classification as the interplay between soil physical properties such as texture (content between 5–30 cm, two layers) and saturated hydraulic conductivity up to 100 cm, which are known to be depth-dependent and dependent on the soil moisture content.

The quality of the results achieved for the Southern Andes landslide assessment using machine-learning classifiers must be considered in light of the inherent variations in density information and database quality. Previous studies in South America encourage improving the landslide database and its controlling factors due to reduced records along history (Fustos-Toribio et al., 2022; Sepúlveda and Petley, 2015). Moreover, no unique classifier method guarantees optimal performance for all datasets; model performance is heavily influenced by the distribution and quality of the input data (Gu et al., 2024). The presented results reveal that, while all classifiers delivered strong performance, nuances such as the slight improvement for SVM under PUBagging and the marginal reduction of accuracy for Random Forest in the same condition underscore the sensitivity of these methods to changes in data handling and sampling strategies. Our findings demonstrate that a promising classifier can achieve effective performance even with a limited database when supported by robust density information and high-quality underlying data (Table 5).

Although the similar performance of GA–RF and GA–XGB, they differ in practical trade-offs. GA–RF is computationally lighter and easier to interpret, favoring operational applications, while GA–XGB is less interpretable but more robust in heterogeneous environments, as it may capture more complex interactions. This complementary perspective may underscore the importance of applying ensemble classifiers for operational landslide forecasting.

Random Forest classifier demonstrates the highest recall in the Non PUBagging condition, achieving 0.879 accuracy and 0.901 recall. It appears to be the more robust choice for landslide susceptibility mapping in regions where data quality is consistent. Although the difference is not significant, its slight performance reduction in the PUBagging scenario suggests that in heterogeneous environments, it may be beneficial to consider additional strategies to mitigate variability. Techniques such as ensemble stacking or hybrid integration, which capitalise on the strengths of multiple algorithms, could further enhance predictive performance, as shown in other studies (Huang et al., 2022). Therefore, while Random Forest seems preferable based on current evidence, an adaptive framework that dynamically incorporates ensemble methods might better serve the Southern Andes, where environmental conditions and data quality may fluctuate (Gu et al., 2024).

However, the limitations of this study are related to the fact that the model performance is conditioned by inventory completeness and by the strong spatial concentration of records, which may limit transferability beyond the most represented regions. In addition, correlations among depth-dependent soil variables and potential spatial autocorrelation can inflate apparent performance if not controlled through spatially independent validation. Finally, the static predictors used here may not fully capture short-term hydrological transients preceding landslides, and uncertainty quantification remains limited. These aspects should be addressed through expanded inventories, spatial cross-validation, and incorporation of near-real-time hydrometeorological observations.

6.3 Future scope

The impact of climate change on mass wasting events cannot be ignored. Recent studies showed evidence that increased precipitation and temperature fluctuations significantly affect sediment yield and debris flow activity in alpine regions (Hirschberg et al., 2021). Future changes in precipitation patterns will urge the implementation of a monitoring framework that incorporates climatic variables alongside geotechnical measurements to adapt to changing conditions effectively.

The necessity for broader monitoring networks with well-defined variables is paramount in the context of rainfall-induced landslides. Rainfall-induced landslides are predominantly triggered by prolonged and intense rainfall, which underscores the importance of capturing detailed hydrological and geological data to enhance predictive capabilities (Li et al., 2021; Fusco et al., 2022). A comprehensive monitoring system that includes variables such as soil moisture, pore water pressure, and rainfall intensity can significantly improve the understanding of slope stability dynamics and the conditions leading to landslide initiation (Abraham et al., 2020; Segoni et al., 2018). For instance, the integration of hydrological monitoring with rainfall data has been shown to refine rainfall thresholds for landslide forecasting, thereby enabling more accurate early warning systems (Teza et al., 2022; Vaz et al., 2018).

Moreover, implementing advanced technologies, such as remote sensing and machine learning, can facilitate real-time data collection and analysis, allowing for timely interventions in high-risk areas (Mondini et al., 2023; Froude and Petley, 2018). However, as stated before, while the proposed classifiers showed strong performance (Abraham et al., 2019; Qiao et al., 2020), their effectiveness is constrained by the quality of the database, which in this domain is challenged by data scarcity, sparsity, and features availability. This affects that the models may not readily generalise to other regions, or even fully capture the evolving dynamics within the study area. Finally, their limited transparency underscores the need for further validation and for integration with physically based models to enhance interpretability and reliability, in particular to consider the meteorological dynamics. Thus, future work should focus on validating these models across diverse regions and integrating them with physically based approaches to enhance both their robustness and interpretability. Additionally, establishing a network of monitoring stations across diverse geomorphological environments can provide valuable insights into the varying responses of slopes to rainfall, thereby improving the generalisability of predictive models (Kuradusenge et al., 2020; Bortolozo et al., 2024).

7 Conclusions

We evaluated machine learning models (SVM, RF and XGB) to predict landslide susceptibility in the southern Andes (38–42° S), selecting domain-relevant geotechnical, hydrological, and geomorphological variables through feature selection techniques (CART and GA). The GA–optimised models, particularly GA-RF and GA-XGB, significantly outperformed baseline methods, achieving the lowest classification errors (10.95 %) with compact feature sets that improved both accuracy and efficiency. Across experiments, slope, precipitation, and near-surface soil hydraulic properties – especially bulk density and saturated water content – emerged as the most critical factors influencing rainfall-induced landslides, underscoring their importance for future monitoring and assessment.

Our findings also underscore the importance of incorporating both shallow and deep soil moisture characteristics, as well as soil retention curve parameters, to better capture the complex subsurface dynamics that precede slope failure. The differences in feature prioritisation between GA-RF, GA-XGB, and GA-SVM reflect distinct modelling philosophies: while RF and XGB emphasised shallow hydraulic traits and retention thresholds, SVM gave greater weight to deeper soil moisture indicators and retention curve shape parameters.

From an operational early warning perspective, the compact GA-selected feature sets reduce monitoring complexity by prioritising a small number of high-impact variables (precipitation, slope, and depth-specific soil hydraulic/moisture indicators). This supports more cost-effective station design and variable selection, while maintaining low error rates. The identified shallow-versus-deep moisture controls also provide guidance for sensor placement (near-surface and deeper soil moisture) in mountainous catchments prone to rainfall-triggered failures.

We conclude that integrating data-driven models with physically meaningful features provides a robust framework for enhancing early warning systems and regional risk assessments. The superior performance of GA-optimised ensemble models suggests that future efforts should prioritise hybrid strategies that combine expert knowledge with automated feature selection. These approaches are particularly valuable in data-scarce environments, offering scalable solutions to inform risk management and decision-making in mountainous regions vulnerable to rainfall-triggered landslides.

Despite the limitations related to the spatial reproducibility of the results, the main contribution of this work lies in proposing a method that can be scaled according to data availability and applied to region-specific contexts, enabling the identification of meaningful variable sets for areas with similar geological or climatic conditions.

Code availability. The code used for feature selection and classification is available upon request from the corresponding author.

Data availability. The landslide database and soil property data are available from the Chilean National Geology and Mining Service (SERNAGEOMIN) and CLSoilMaps database respectively. Climate data from ERA5-land is publicly available through the Copernicus Climate DataStore (https://doi.org/10.24381/cds.e2161bac, Copernicus Climate Change Service, 2019).

Author contributions. All authors contributed to the study conception and design. Data collection, depuration and analysis were performed by [Ivo Fustos and Millaray Curilem]. Machine learning implementation was carried out by [Manuel Labbé]. Geological interpretation was 480 provided by [Ivo Fustos and Mario Pooley]. All authors contributed to the writing and revision of the manuscript.

Competing interests. The contact author has declared that none of the authors has any competing interests.

Disclaimer. Publisher's note: Copernicus Publications remains neutral with regard to jurisdictional claims made in the text, published maps, institutional affiliations, or any other geographical representation in this paper. The authors bear the ultimate responsibility for providing appropriate place names. Views expressed in the text are those of the authors and do not necessarily reflect the views of the publisher.

Special issue statement. This article is part of the special issue "The influence of landslide inventory quality on susceptibility and hazard map reliability". It is a result the EGU General Assembly 2024, session NH3.10 "Exploring the Interplay: Quality of Landslide Inventories and reliability of Susceptibility and Hazard mapping", Vienna, Austria, 19 April 2024.

Acknowledgements. We thank the Chilean National Geology and Mining Service (SERNAGEOMIN) for providing the landslide database through the Xterrae platform. We also acknowledge the Copernicus Climate Data Store for ERA5-land data and the CLSoilMaps project for soil property data. This research was supported by FONDEF ID23i10118 and Fondecyt Regular grant 1230792. The authors sincerely acknowledge the substantial contributions of Bei Zhang, one anonymous and Dr Federica Fiorucci throughout the review process. Their insightful comments, constructive suggestions, and careful evaluation greatly improved the quality, clarity, and scientific rigour of this manuscript. The authors are deeply grateful for the time and expertise they dedicated to this work.

Financial support. This research has been supported by the Agencia Nacional de Investigación y Desarrollo (grant nos. 1230792 and ID23i10118).

Review statement. This paper was edited by Federica Fiorucci and reviewed by Bei Zhang and one anonymous referee.

References

Abraham, M., Pothuraju, D., and Satyam, N.: Rainfall thresholds for prediction of landslides in idukki, india: an empirical approach, Water, 11, 2113, https://doi.org/10.3390/w11102113, 2019.

Abraham, M., Satyam, N., Kushal, S., Rosi, A., Pradhan, B., and Segoni, S.: Rainfall threshold estimation and landslide forecasting for kalimpong, india using sigma model, Water, 12, 1195, https://doi.org/10.3390/w12041195, 2020.

Adnan, M., Rahman, M., Ahmed, N., Ahmed, B., Rabbi, M., and Rahman, R.: Improving spatial agreement in machine learning-based landslide susceptibility mapping, Remote Sens., 12, 3347, https://doi.org/10.3390/rs12203347, 2020.

Ballabh, H., Pillay, S., Negi, G., and Pillay, K.: Relationship between selected physiographic features and landslide occurrence around four hydropower projects in bhagirathi valley of uttarakhand, western himalaya, india, Int. J. Geosci., 5, 1088–1099, https://doi.org/10.4236/ijg.2014.510093, 2014.

Barnhart, K. R., George, D. L., Collins, A. L., Schaefer, L. N., and Staley, D. M.: Uncertainty Reduction for Subaerial Landslide-Tsunami Hazards, J. Geophys. Res.-Earth, 130, https://doi.org/10.1029/2024jf007906, 2025.

Bezak, N., Auflic, M., and Mikoš, M.: Application of hydrological modelling for temporal prediction of rainfall-induced shallow landslides, Landslides, 16, 1273–1283, https://doi.org/10.1007/s10346-019-01169-9, 2019.

Bisht, S. and Rawat, K.: A review of statistical approaches used for landslide susceptibility analysis with the help of remote sensing and gis technology, Acta Scientiarum Polonorum Formatio Circumiectus, 22, 83–96, https://doi.org/10.15576/asp.fc/2023.22.3.13, 2023.

Bonshoms, M., Ubeda, J., Liguori, G., Körner, P., Navarro, Á., and Cruz, R.: Validation of ERA5-Land temperature and relative humidity on four Peruvian glaciers using on-glacier observations, J. Mt. Sci., 19, 1849–1873, https://doi.org/10.1007/s11629-022-7388-4, 2022.

Bordoni, M., Meisina, C., Valentino, R., Lu, N., Bittelli, M., and Chersich, S.: Hydrological factors affecting rainfall-induced shallow landslides: from the field monitoring to a simplified slope stability analysis, Eng. Geol., 193, 19–37, https://doi.org/10.1016/j.enggeo.2015.04.006, 2015.

Bortolozo, C. A., Pampuch, L. A., de Andrade, M. R. M., Metodiev, D., Carvalho, A. R., Mendes, T. S. G., Pryer, T., Egas, H. M., Mendes, R. M., Sousa, I. A., and Power, J.: Arhcs (automatic rainfall half-life cluster system): a landslides early warning system (lews) using cluster analysis and automatic threshold definition, Int. J. Geosci., 15, 54–69, https://doi.org/10.4236/ijg.2024.151005, 2024.

Bravo-López, P., Fernández, T., Sellers, C., and García, J.: Analysis of conditioning factors in cuenca, ecuador, for landslide susceptibility maps generation employing machine learning methods, Land, 12, 1135, https://doi.org/10.3390/land12061135, 2023.

Chen, T.-H. K., Kincey, M. E., Rosser, N. J., and Seto, K. C.: Identifying recurrent and persistent landslides using satellite imagery and deep learning: A 30-year analysis of the Himalaya, Sci. Total Environ., 922, 171161, https://doi.org/10.1016/j.scitotenv.2024.171161, 2024.

Copernicus Climate Change Service (C3S): ERA5-Land hourly data from 1950 to present, Copernicus Climate Change Service (C3S) Climate Data Store (CDS) [data set], https://doi.org/10.24381/cds.e2161bac, 2019.

Crozier, M.: Deciphering the effect of climate change on landslide activity: a review, Geomorphology, 124, 60–267, https://doi.org/10.1016/j.geomorph.2010.04.009, 2010.

Cuzzone, J., Romero, M., and Marcott, S. A.: Modeling the timing of Patagonian Ice Sheet retreat in the Chilean Lake District from 22–10 ka, The Cryosphere, 18, 1381–1398, https://doi.org/10.5194/tc-18-1381-2024, 2024.

Dinamarca, D. I., Galleguillos, M., Seguel, O., and Faúndez-Urbina, C.: CLSoilMaps: A comprehensive soil property database for Chile, Soil Sci. Soc. Am. J., 87, 345–358, https://doi.org/10.1038/s41597-023-02536-x, 2023.

Ebrahimi Warkiani, M. and Moattar, M. H.: A comprehensive survey on recent feature selection methods for mixed data: Challenges, solutions and future directions, Neurocomputing, 623, 129372, https://doi.org/10.1016/j.neucom.2025.129372, 2025.

Emberson, R., Kirschbaum, D. B., Amatya, P., Tanyas, H., and Marc, O.: Insights from the topographic characteristics of a large global catalog of rainfall-induced landslide event inventories, Nat. Hazards Earth Syst. Sci., 22, 1129–1149, https://doi.org/10.5194/nhess-22-1129-2022, 2022.

Fidan, S., Tanyaş, H., Akbaş, A., Lombardo, L., Petley, D. N., and Görüm, T.: Understanding fatal landslides at global scales: a summary of topographic, climatic, and anthropogenic perspectives, Nat. Hazards, 120, 6437–6455, https://doi.org/10.1007/s11069-024-06487-3, 2024.

Froude, M. J. and Petley, D. N.: Global fatal landslide occurrence from 2004 to 2016, Nat. Hazards Earth Syst. Sci., 18, 2161–2181, https://doi.org/10.5194/nhess-18-2161-2018, 2018.

Fusco, F., Bordoni, M., Tufano, R., Vivaldi, V., Meisina, C., Valentino, R., Bittelli, M., and De Vita, P.: Hydrological regimes in different slope environments and implications on rainfall thresholds triggering shallow landslides, Nat. Hazards, 114, 907–939, https://doi.org/10.1007/s11069-022-05417-5, 2022.

Fustos-Toribio, I. J., Morales-Vargas, B., Somos-Valenzuela, M., Moreno-Yaeger, P., Muñoz-Ramirez, R., Rodriguez Araneda, I., and Chen, N.: Debris flow event on Osorno volcano, Chile, during summer 2017: new interpretations for chain processes in the southern Andes, Nat. Hazards Earth Syst. Sci., 21, 3015–3029, https://doi.org/10.5194/nhess-21-3015-2021, 2021.

Fustos-Toribio, I., Manque-Roa, N., Vásquez Antipan, D., Hermosilla Sotomayor, M., and Letelier Gonzalez, V.: Rainfall-induced landslide early warning system based on corrected mesoscale numerical models: an application for the southern Andes, Nat. Hazards Earth Syst. Sci., 22, 2169–2183, https://doi.org/10.5194/nhess-22-2169-2022, 2022.

Fustos-Toribio, I., Basualto, D., Gatica, A., Bravo-Alarcón, A., Palma, J.-L., Fuentealba, G., and Sepúlveda, S. A.: Controls over debris flow initiation in glacio-volcanic environments in the Southern Andes, Nat. Hazards Earth Syst. Sci., 25, 4843–4861, https://doi.org/10.5194/nhess-25-4843-2025, 2025.

Gariano, S. L., Petrucci, O., and Guzzetti, F.: Changes in the occurrence of rainfall-induced landslides in Calabria, southern Italy, in the 20th century, Nat. Hazards Earth Syst. Sci., 15, 2313–2330, https://doi.org/10.5194/nhess-15-2313-2015, 2015.

Ge, Q., Wang, J., Liu, C., Wang, X., Deng, Y., and Li, J.: Integrating Feature Selection with Machine Learning for Accurate Reservoir Landslide Displacement Prediction, Water, 16, 2152, https://doi.org/10.3390/w16152152, 2022.

Gu, T., Duan, P., Wang, M., and et al.: Effects of non-landslide sampling strategies on machine learning models in landslide susceptibility mapping, Sci. Rep., 14, 7201, https://doi.org/10.1038/s41598-024-57964-5, 2024.

Guyon, I. and Elisseeff, A.: An Introduction to Variable and Feature Selection, J. Mach. Learn. Res., 3, 1157–1182, https://doi.org/10.1162/153244303322753616, 2003.

Halder, K., Srivastava, A. K., Ghosh, A., Das, S., Banerjee, S., Pal, S. C., Chatterjee, U., Bisai, D., Ewert, F., and Gaiser, T.: Improving landslide susceptibility prediction through ensemble Recursive Feature Elimination and meta-learning framework, Research Square [preprint], https://doi.org/10.21203/rs.3.rs-3991474/v1, 2024.

Hirschberg, J., Fatichi, S., Bennett, G., McArdell, B., Peleg, N., Lane, S., and van Meerveld, H.: Climate change impacts on sediment yield and debris-flow activity in an alpine catchment, J. Geophys. Res.-Earth, 126, e2020JF005739, https://doi.org/10.1029/2020jf005739, 2021.

Horton, B. K.: Tectonic Regimes of the Central and Southern Andes: Responses to Variations in Plate Coupling During Subduction, Tectonics, 37, 402–429, https://doi.org/10.1002/2017tc004624, 2018.

Huang, F., Cao, Z., Guo, J., Jiang, S.-H., Li, S., and Guo, Z.: Comparisons of heuristic, general statistical and machine learning models for landslide susceptibility prediction and mapping, Catena, 191, 104580, https://doi.org/10.1016/j.catena.2020.104580, 2019.

Huang, F., Chen, J., Liu, W., Huang, J., Hong, H., and Chen, W.: Regional rainfall-induced landslide hazard warning based on landslide susceptibility mapping and a critical rainfall threshold, Geomorphology, 408, 108236, https://doi.org/10.1016/j.geomorph.2022.108236, 2022.

Islam, M., Islam, M., and Jeet, A.: A geotechnical investigation of 2017 Chattogram landslides, Geosciences, 11, 337, https://doi.org/10.3390/geosciences11080337, 2021.

Jia, L., Wang, J., Gao, S., Fang, L., and Wang, D.: Landslide risk evaluation method of open-pit mine based on numerical simulation of large deformation of landslide, Sci. Rep., 13, 15892, https://doi.org/10.1038/s41598-023-42736-4, 2023.

Katoch, S., Chauhan, S. S., and Kumar, V.: A review on genetic algorithm: past, present, and future, Multimed. Tools Appl., 80, 8091–8126, https://doi.org/10.1007/s11042-020-10139-6, 2020.

Kirschbaum, D. and Stanley, T.: Satellite-based assessment of rainfall-triggered landslide hazard for situational awareness, Earth's Future, 6, 505–523, https://doi.org/10.1002/2017ef000715, 2018.

Kumar, C., Walton, G., Santi, P., and Luza, C.. An Ensemble Approach of Feature Selection and Machine Learning Models for Regional Landslide Susceptibility Mapping in the Arid Mountainous Terrain of Southern Peru, Remote Sens., 15, 1376, https://doi.org/10.3390/rs15051376, 2023.

Kuradusenge, M., Kumaran, S., and Zennaro, M.: Rainfall-induced landslide prediction using machine learning models: the case of ngororero district, rwanda, Int. J. Env. Res. Pub. He., 17, 4147, https://doi.org/10.3390/ijerph17114147, 2020.

Li, D., Huang, F., Yan, L., Cao, Z., Chen, J., and Zhou, Y.: Landslide susceptibility prediction using particle-swarm-optimized multilayer perceptron: comparisons with multilayer-perceptron-only, bp neural network, and information value models, Appl. Sci., 9, 3664, https://doi.org/10.3390/app9183664, 2019.

Li, W., Liu, Y., Chen, Y., and Yang, L.: Shock and vibration of rainfall on rotational landslide and analysis of its deformation characteristics, 560 Geofluids, 2021, 4119414, https://doi.org/10.1155/2021/4119414, 2021.

Lin, L., Lin, Q., and Wang, Y.: Landslide susceptibility mapping on a global scale using the method of logistic regression, Nat. Hazards Earth Syst. Sci., 17, 1411–1424, https://doi.org/10.5194/nhess-17-1411-2017, 2017.

Maragaño-Carmona, G., Fustos Toribio, I. J., Descote, P.-Y., Robledo, L. F., Villalobos, D., and Gatica, G.: Rainfall-Induced Landslide Assessment under Different Precipitation Thresholds Using Remote Sensing Data: A Central Andes Case, Water, 15, 2514, https://doi.org/10.3390/w15142514, 2023.

Maragaño-Carmona, G., Fustos-Toribio, I., Moreno-Yaeger, P., Ramirez, E., Basualto, D., Nie, W., Descote, P.-Y., and Robledo, L. F.: Assessment of geomorphological, hydrometeorological and geological trigger conditions of debris flows in northern Patagonia Andes, B. Eng. Geol. Environ., 84, https://doi.org/10.1007/s10064-024-04004-1, 2025.

Maragaño-Carmona, G., Fustos Toribio, I. J., Descote, P.-Y., Robledo, L. F., Villalobos, D., and Gatica, G.: Rainfall-Induced Landslide Assessment under Different Precipitation Thresholds

Using Remote Sensing Data: A Central Andes Case, Water, 15, 2514, https://doi.org/10.3390/w15142514, 2023.

Marc, O., Hovius, N., Meunier, P., Görüm, T., and Uchida, T.: A seismologically consistent expression for the total area and volume of earthquake-triggered landsliding, J. Geophys. Res.-Earth, 121, 640–663, https://doi.org/10.1002/2015jf003732, 2016.

Marc, O., Gosset, M., Saitô, H., Uchida, T., and Malet, J.: Spatial patterns of storm-induced landslides and their relation to rainfall anomaly maps, Geophys. Res. Lett., 46, 11167–11177, https://doi.org/10.1029/2019gl083173, 2019.

McBratney, A. B., Mendonça Santos, M. L., and Minasny, B.: On digital soil mapping, Geoderma, 117, 3–52, https://doi.org/10.1016/s0016-7061(03)00223-4, 2003.

Merghadi, A., Yunus, A. P., Dou, J., Whiteley, J., Thai Pham, B., Bui, D. T., and Avtar, R.: Machine learning methods for landslide susceptibility studies: A comparative overview of algorithm performance, Earth-Sci. Rev., 207, 103225, https://doi.org/10.1016/j.earscirev.2020.103225, 2020.

Mondini, A., Guzzetti, F., and Melillo, M.: Deep learning forecast of rainfall-induced shallow landslides, Nat. Commun., 14, 2466, https://doi.org/10.1038/s41467-023-38135-y, 2023.

Moreno-Yaeger, P., Singer, B. S., Edwards, B. R., Jicha, B. R., Nachlas, W. O., Kurz, M. D., E. Breunig, R., Fustos-Toribio, I., Antipán, D. V., and Piergrossi, E.: Pleistocene to recent evolution of Mocho-Choshuenco volcano during growth and retreat of the Patagonian Ice Sheet, Geol. Soc. Am. Bull., 136, 5262–5282, https://doi.org/10.1130/b37514.1, 2024.

Muñoz-Sabater, J., Dutra, E., Agustí-Panareda, A., Albergel, C., Arduini, G., Balsamo, G., Boussetta, S., Choulga, M., Harrigan, S., Hersbach, H., Martens, B., Miralles, D. G., Piles, M., Rodríguez-Fernández, N. J., Zsoter, E., Buontempo, C., and Thépaut, J.-N.: ERA5-Land: a state-of-the-art global reanalysis dataset for land applications, Earth Syst. Sci. Data, 13, 4349–4383, https://doi.org/10.5194/essd-13-4349-2021, 2021.

NASA Jet Propulsion Laboratory: NASA Shuttle Radar Topography Mission Global 1 arc second, NASA Land Processes Distributed Active Archive Center, https://doi.org/10.5067/MEASURES/SRTM/SRTMGL1.003, 2013.

Nielsen, K. T., Moldrup, P., Thorndahl, S., Nielsen, J. E., Uggerby, M., and Rasmussen, M. R.: Field-Scale Monitoring of Urban Green Area Rainfall-Runoff Processes, J. Hydrol. Eng., 24, https://doi.org/10.1061/(asce)he.1943-5584.0001795, 2019.

Novellino, A., Cesarano, M., Cappelletti, P., Di Martire, D., Di Napoli, M., Ramondini, M., Sowter, A., and Calcaterra, D.: Slow-moving landslide risk assessment combining machine learning and insar techniques, Catena, 203, 105317, https://doi.org/10.1016/j.catena.2021.105317, 2021.

Ochoa-Cornejo, F., Palma, S., Sepúlveda, S. A., Lara, M., Burgos, K., and Duhart, P.: Rock slides in paraglacial environments in South America: three-dimensional modeling of glacier retreat and landslide inducing the 2017 Santa Lucía disaster in the Chilean Patagonia, Landslides, 22, 1003–1025, https://doi.org/10.1007/s10346-024-02419-1, 2025.

Oh, S., Kim, Y., and Kim, J.-W.: A Modified van Genuchten-Mualem Model of Hydraulic Conductivity in Korean Residual Soils, Water, 7, 5487–5502, https://doi.org/10.3390/w7105487, 2015.

Park, S. and Kim, J.: Landslide susceptibility mapping based on random forest and boosted regression tree models, and a comparison of their performance, Appl. Sci., 9, 942, https://doi.org/10.3390/app9050942, 2019.

Peranić, J., Čeh, N., and Arbanas, Ž.: The Use of Soil Moisture and Pore-Water Pressure Sensors for the Interpretation of Landslide Behavior in Small-Scale Physical Models, Sensors, 22, 7337, https://doi.org/10.3390/s22197337, 2022.

Pham, B. T., Phong, T. V., Avand, M., Al-Ansari, N., Singh, S. K., Le, H. V., and Prakash, I.: Improving voting feature intervals for spatial prediction of landslides, Math. Probl. Eng., 2020, 4310791, https://doi.org/10.1155/2020/4310791, 2020.

Qiao, S., Feng, C., Yu, P., Tan, J., Uchimura, T., Wang, L., Tang, J., Shen, Q., and Xie, J.: Investigation on surface tilting in the failure process of shallow landslides, Sensors, 20, 2662, https://doi.org/10.3390/s20092662, 2020.

Segoni, S., Rosi, A., Lagomarsino, D., Fanti, R., and Casagli, N.: Brief communication: Using averaged soil moisture estimates to improve the performances of a regional-scale landslide early warning system, Nat. Hazards Earth Syst. Sci., 18, 807–812, https://doi.org/10.5194/nhess-18-807-2018, 2018.

Sepúlveda, S. A. and Petley, D. N.: Regional trends and controlling factors of fatal landslides in Latin America and the Caribbean, Nat. Hazards Earth Syst. Sci., 15, 1821–1833, https://doi.org/10.5194/nhess-15-1821-2015, 2015.

Somos-Valenzuela, M. A., Oyarzún-Ulloa, J. E., Fustos-Toribio, I. J., Garrido-Urzua, N., and Chen, N.: The mudflow disaster at Villa Santa Lucía in Chilean Patagonia: understandings and insights derived from numerical simulation and postevent field surveys, Nat. Hazards Earth Syst. Sci., 20, 2319–2333, https://doi.org/10.5194/nhess-20-2319-2020, 2020.

Song, Y.-W., Wang, J.-S., Qi, Y.-L., Wang, Y.-C., Song, H.-M., and Shang-Guan, Y.-P.: Serial filter-wrapper feature selection method with elite guided mutation strategy on cancer gene expression data, Artif. Intell. Rev., 58, https://doi.org/10.1007/s10462-024-11029-1, 2025.

Steger, S., Moreno, M., Crespi, A., Zellner, P. J., Gariano, S. L., Brunetti, M. T., Melillo, M., Peruccacci, S., Marra, F., Kohrs, R., Goetz, J., Mair, V., and Pittore, M.: Deciphering seasonal effects of triggering and preparatory precipitation for improved shallow landslide prediction using generalized additive mixed models, Nat. Hazards Earth Syst. Sci., 23, 1483–1506, https://doi.org/10.5194/nhess-23-1483-2023, 2023.

Tetzner, D. R., Allen, C. S., Thomas, E. R., Wolff, E. W., and Franzke, C. L. E.: Timing of the Recent Migration and Intensification of the Southern Hemisphere Westerly Winds, Geophys. Res. Lett., 52, https://doi.org/10.1029/2024gl113672, 2025.

Teza, G., Cola, S., Brezzi, L., and Galgaro, A.: Wadenow: a matlab toolbox for early forecasting of the velocity trend of a rainfall-triggered landslide by means of continuous wavelet transform and deep learning, Geosciences, 12, 205, https://doi.org/10.3390/geosciences12050205, 2022.

Theng, D. and Bhoyar, K. K.: Feature selection techniques for machine learning: a survey of more than two decades of research, Knowl. Inf. Syst., 66, 1575–1637, https://doi.org/10.1007/s10115-023-02010-5, 2024.

Vásquez-Antipán, D., Fustos-Toribio, I., Riffo-López, J., Cortez-Díaz, A., Bravo, Á., and Moreno-Yaeger, P.: Landslide processes related to recurrent explosive eruptions in the Southern Andes of Chile (39° S), J. S. Am. Earth Sci., 157, 105469, https://doi.org/10.1016/j.jsames.2025.105469, 2025.

Vaz, T., Zêzere, J. L., Pereira, S., Oliveira, S. C., Garcia, R. A. C., and Quaresma, I.: Regional rainfall thresholds for landslide occurrence using a centenary database, Nat. Hazards Earth Syst. Sci., 18, 1037–1054, https://doi.org/10.5194/nhess-18-1037-2018, 2018.

Vorpahl, P., Dislich, C., Elsenbeer, H., Märker, M., and Schröder, B.: Biotic controls on shallow translational landslides, Earth Surf. Proc. Land., 38, 198–212, https://doi.org/10.1002/esp.3320, 2012.

Wang, X., Wang, Y., Lin, Q., and Yang, X.: Assessing global landslide casualty risk under moderate climate change based on multiple gcm projections, Int. J. Disast. Risk Sc., 14, 751–767, https://doi.org/10.1007/s13753-023-00514-w, 2023.

Wang, Z., Wang, D., Guo, Q., and Wang, D.: Regional landslide hazard assessment through interating susceptibility index and rainfall process, Nat. Hazards, 104, 2153–2173, https://doi.org/10.1007/s11069-020-04265-5, 2020.

Wu, B., Qiu, W., Jia, J., and Liu, N. Landslide susceptibility modeling using bagging-based positive–unlabeled learning, IEEE Geosci. Remote S., 18, 766–770, https://doi.org/10.1109/LGRS.2020.2989497, 2021.

Xu, Y., Dai, Q., Zhu, J., Yao, Y., Zhang, J., Li, W., Han, D., Zhu, S., Zeng, T., Xu, Y., and Han, D.: Increased significance of global concurrent hazards from 1981 to 2020, Earth's Future, 12, e2024EF004490, https://doi.org/10.1029/2024ef004490, 2024.

Yang, K., Niu, R., Song, Y., Dong, J., Zhang, H., and Chen, J.: Dynamic hazard assessment of rainfall-induced landslides using gradient boosting decision tree with google earth engine in three gorges reservoir area, china, Water, 16, 1638, https://doi.org/10.3390/w16121638, 2024.

Yilmaz, M.: Accuracy assessment of temperature trends from ERA5 and ERA5-Land, Sci. Total Environ., 856, 159182, https://doi.org/10.1016/j.scitotenv.2022.159182, 2023.

Zhang, Y. and Schaap, M. G.: Weighted recalibration of the Rosetta pedotransfer model with improved estimates of hydraulic parameter distributions and summary statistics (Rosetta3), J. Hydrol., 547, 39–53, https://doi.org/10.1016/j.jhydrol.2017.01.004, 2017.

Zheng, A. and Casari, A.: Feature Engineering for Machine Learning: Principles and Techniques for Data Scientists, O'Reilly Media, Sebastopol, ISBN 13 978-1491953242, 2021.

Zighmi, K., Zahri, F., Faqeih, K., Al Amri, A., Riheb, H., Alamri, S. M., and Alamery, E.: AHP multi criteria analysis for landslide susceptibility mapping in the Tellian Atlas chain, Sci. Rep., 15, https://doi.org/10.1038/s41598-025-10819-z, 2025.